

Phase field modelling of the detachment of bubbles from a solid substrate

Carlos Uriarte

Área de Electromagnetismo, Universidad Rey Juan Carlos,
Tulipán s/n, Mostoles, 28933, Madrid, Spain

Marco A. Fontelos

Instituto de Ciencias Matemáticas (ICMAT, CSIC-UAM-UC3M-
UCM), C/ Nicolás Cabrera 15, 28049 Madrid, Spain.

Manuel Arrayás

Área de Electromagnetismo, Universidad Rey Juan Carlos,
Tulipán s/n, Mostoles, 28933, Madrid, Spain

March 20, 2024

Abstract

We develop and implement numerically a phase field model for the evolution and detachment of a gas bubble resting on a solid substrate and surrounded by a viscous liquid. The bubble has a static contact angle θ and will be subject to gravitational forces. We compute, as a function of the static contact angle, the critical Bond number over which bubbles detach from the substrate. Then, we perform similar studies for bubble resting on inclined substrates and bubbles under the action of an external flow. We provide approximate formulas for the critical Bond number under all these circumstances. Our method is also able to resolve the pinchoff of the bubble and the possible appearance of satellites.

1 Introduction

The nucleation, growth and detachment of gas bubbles surrounded by a viscous liquid is a classical problem in fluid mechanics. It appears in contexts as diverse as boiling of liquids (cf. [15]), cavitation (cf. [12]), bubble creation and transport in microchannels (cf. [11]) or electrochemistry (cf. [10]). In the context of electrochemistry, where chemical reactions at an electrode can lead to the production of molecules in a gas phase so that bubbles nucleate and grow attached to it. When the bubble's volume is sufficiently large, the bubble can detach

and carry the produced gas with it. This is the case, for instance, of Hydrogen produced by electrolysis of water which is a process of enormous industrial importance in connection to the storage and transport of energy produced by renewable means such as solar and wind energies (see for instance [18]). It is then natural to search for methods and techniques to optimize the processes of electrolysis in order to increase energy production (cf. [13]).

The life cycle of a bubble at a gas-evolving electrode begins with its nucleation at a suitable site of the electrode surface. The bubble grows by taking up dissolved gas that reaches its surface by diffusion, and detaches from the electrode when the buoyancy force, aided by hydrodynamic forces if the liquid flows around the electrode, overcomes the surface tension and electric forces that keep the bubble attached to the electrode surface. The detached bubble then drifts in the liquid until it reaches the surface where the gas is collected. Coalescence of bubbles may occur before and after detachment. The main difficulty when modelling a bubble and its detachment is the presence of moving interfaces (the surface of the bubble) separating different media. This forces the implementation of suitable boundary conditions at a surface that evolves in time. A useful approach to simulation of problems involving moving interfaces separating two different phases is by means of a so-called phase field (see [3], [4] for a general description of the method and [5], [6], [8], [7], [9] for its application for fluid mechanical problems). The phase field approach replaces (in a way to be described below) the sharp interface by a so-called diffuse interface across which a phase field function changes smoothly. This removes the difficulty of numerically tracking the interface which is replaced by a suitable level surface of the phase field (cf. [4]). In addition, one can handle topological changes such as those produced in the detachment or coalescence of bubbles (see [10]).

In this article we implement and use a phase field model for the growth and detachment of gas bubbles from a solid substrate under various circumstances represented in figure 1. Section 2 will be devoted to the deduction of a suitable phase field model coupling with Navier-Stokes equations and being able to resolve a predetermined contact angle condition. In section 3 we will use this model to study the evolution and stability of bubbles of different volumes (more precisely, for different Bond numbers). In section 4 we consider the situation of an inclined substrate on bubble detachment. Finally, in section 4 we impose an external flow and study its influence in bubble detachment. We will develop a phase plane for bubble detachment conditions as a function of both volume and imposed external flow and will do it for multiple contact angles.

2 Phase field modelling

One of the most effective methods to study multiphase flows is the so-called phase field method. The main idea is to replace sharp interfaces by “diffuse” interfaces where a phase field function $\phi(\mathbf{x}, t)$ experiences sharp transitions (across the diffuse interface with a thickness of order ε sufficiently small) between to

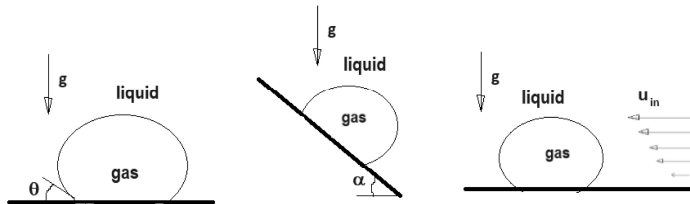


Figure 1: Sketch of physical settings: bubble under gravity (left), over a inclined substrabe (center) and under external flow and gravity (right). θ is the contact angle and α the inclination angle.

limiting values (say $\phi = 1$ and $\phi = -1$, for instance) corresponding to two different fluids. The introduction of diffuse interfaces has, as one of its main advantages, the property that topological changes in the different fluid domains can be dealt with easily. One needs to provide a suitable PDE to the phase field $\phi(\mathbf{x}, t)$ and couple to other fluid variables in a proper way. This has been studied in many papers (cf. [5], [6], [8], [7], [9] for instance). For the phase field function, the suitable equation is a fourth order PDE called the Cahn-Hilliard equation (firstly introduced in [2], see also [1]) including a convection term with a velocity $\mathbf{v}(\mathbf{x}, t)$ which is the fluid velocity:

$$\frac{\partial \phi}{\partial t} + \mathbf{v} \cdot \nabla \phi = \nabla \cdot (M \nabla \psi), \quad (1)$$

with

$$\psi = -\varepsilon \Delta \phi + \frac{1}{\varepsilon} W(\phi), \quad (2)$$

where ψ is the so-called chemical potential.

In (1) M is a “mobility” factor and in (2) $W(\phi)$ is a phase-field potential with the property of having two local minima at values of ϕ corresponding to the two phases. In particular we will take $W(\phi) = \phi^2(1 - \phi^2)$.

Concerning Navier-Stokes system, we have

$$\frac{\partial(\rho(\phi) \mathbf{v})}{\partial t} + \rho(\phi) \mathbf{v} \cdot \nabla \mathbf{v} - \nabla \cdot \mathbf{S} = -\nabla p + \mu \nabla \phi - \rho(\phi) g \mathbf{e}_z,$$

where the viscous stress tensor is given by

$$\mathbf{S} = \frac{\mu(\phi)}{2} (\nabla \mathbf{v} + \nabla \mathbf{v}^T),$$

and the material parameters $\rho(\phi)$ and $\mu(\phi)$ interpolate between the fluids densities and viscosities respectively:

$$\begin{aligned} \rho(\phi) &= \rho_1 \phi + \rho_2 (1 - \phi), \\ \mu(\phi) &= \mu_1 \phi + \mu_2 (1 - \phi). \end{aligned}$$

We will also assume fluid incompressibility:

$$\nabla \cdot \mathbf{v} = 0,$$

and for the phase field the boundary condition

$$\frac{\partial \psi}{\partial n} = 0. \quad (3)$$

The condition (3) is not sufficient for a fourth order equation such as (1) and we need another boundary condition. Following [7] and [8], we will impose the condition

$$\sigma_0 \varepsilon \frac{\partial \phi}{\partial n} = \sigma'_{fs}(\phi), \quad (4)$$

where $\sigma'_{fs}(\phi)$ interpolates between the liquid/solid interfacial energy σ_{LS} and the gas/solid interfacial energy σ_{GS} :

$$\sigma'_{fs}(\phi) = \frac{\sigma_{GS} + \sigma_{LS}}{2} + \frac{\sigma_{GS} - \sigma_{LS}}{2} \sin\left(\frac{\pi \phi}{2}\right),$$

and σ_0 is proportional to the liquid/gas interfacial energy σ_{LG} :

$$\sigma_0 = \frac{3\sqrt{2}}{8} \sigma_{LG}.$$

In this way, the condition (4) imposes, in the limit $\varepsilon \rightarrow 0$, a liquid/gas contact (or Young's) angle θ_Y such that

$$\cos \theta_Y = \frac{\sigma_{GS} - \sigma_{LS}}{\sigma_{LG}}.$$

The phase field model described in this section has been implemented numerically by means of a finite element method implemented in COMSOL. The initial bubble has a radius $r = 1$ (dimensionless units) and lied inside a computational rectangular box of size $10 \times 10 \times 20$ dimensionless units. The computational domain has been discretized by using approximately $N = 2.3 \times 10^6$ elements.

3 Transient evolution and stability/instability

In this section we will study the evolution and detachment (or not) of a bubble on a solid substrate and inside a viscous liquid. We will base our theoretical discussion on the sharp interface description and present numerical results for the diffuse interface approximation.

$$\frac{\partial(\rho_i \mathbf{v})}{\partial t} + \rho_i \mathbf{v} \cdot \nabla \mathbf{v} - \nabla \cdot \mathbf{S}_i = -\nabla p - \rho_i g \mathbf{e}_z,$$

with a viscous stress

$$\mathbf{S}_i = \frac{\mu_i}{2} (\nabla \mathbf{v} + \nabla \mathbf{v}^T),$$

and the balance of force condition at the interface

$$[(-p\mathbf{I} + \mathbf{S}_i) \cdot \mathbf{n}] = \sigma \kappa \mathbf{n},$$

where $\kappa(\mathbf{x}, t)$ is the mean curvature at any point \mathbf{x} at the surface of the bubble in contact with the liquid and σ represents the surface tension between the liquid and gas interfaces. We consider, as initial data, a bubble consisting of a half-sphere with radius R . Note that R may be related to the volume V of the bubble by means of the relation

$$V = \frac{2}{3} \pi R^3.$$

The introduction of a characteristic velocity U defined from the following balance between inertial and gravitational forces

$$\rho_1 \frac{U^2}{R} = \rho_1 g,$$

allows to write the system in terms of the following dimensionless numbers

$$Bo = \frac{gR^2 \rho_1}{\sigma}, \quad Re = \frac{\rho U R}{\mu},$$

where Bo is the Bond number and Re the Reynolds number, as well as the density and viscosity ratios

$$\gamma = \frac{\rho_2}{\rho_1}, \quad \delta = \frac{\mu_2}{\mu_1}.$$

Hence, the velocity field satisfies

$$\begin{aligned} \frac{\partial \mathbf{v}}{\partial t} + \mathbf{v} \cdot \nabla \mathbf{v} - \frac{1}{Re} \Delta \mathbf{v} &= -\nabla p - Bo \mathbf{e}_z, \quad \text{in the liquid phase,} \\ \frac{\partial \mathbf{v}}{\partial t} + \mathbf{v} \cdot \nabla \mathbf{v} - \frac{\delta}{Re} \Delta \mathbf{v} &= -\nabla p - \gamma Bo \mathbf{e}_z, \quad \text{in the gas phase.} \end{aligned}$$

We are going to compare the energy of a detached bubble with the energy of a bubble attached to a solid substrate. No external flow is considered. There are two energies to consider: 1) Interfacial energies

$$\begin{aligned} E_s &= \sigma_{LG}A_{LG} + \sigma_{LS}A_{LS} + \sigma_{GS}A_{GS} \\ &= \sigma_{LG}A_{LG} + \sigma_{LS}(A_S - A_{GS}) + \sigma_{GS}A_{GS} \\ &= C + \sigma_{LG}A_{LG} + (\sigma_{GS} - \sigma_{LS})A_{GS}, \end{aligned}$$

where A_{LG} , A_{LS} and A_{GS} are the liquid/gas, liquid/solid and gas/solid interfacial areas respectively and σ_{LG} , σ_{LS} and σ_{GS} the corresponding surface tension coefficients. The constant $C = \sigma_{LS}A_S$ is the interfacial energy when the liquid wets the whole solid substrate (with area A_S). The energy with the bubble detached is

$$E_s^d = C + \sigma_{LG}A_{LG}^d.$$

We can approximate, for small contact angles (measured in the liquid phase),

$$A_{LG}^d \simeq A_{LG} + A_{GS}.$$

Hence, since

$$\frac{\sigma_{GS} - \sigma_{LS}}{\sigma_{LG}} = \cos \theta,$$

we have

$$\Delta E_s = \sigma_{LG}(1 - \cos \theta)A_{GS}.$$

We compute now the potential energy. Concerning the detached bubble (assumed spherical and of radius r), it is

$$E_p^d = (\rho_L - \rho_G)gVr,$$

while for the attached bubble

$$E_p = (\rho_L - \rho_G)gV(r - \delta h),$$

where δh is the difference in height between a spherical detached bubble and an attached spherical cap with contact angle θ . The difference in potential energy is, up to $O(\delta h^2)$ error,

$$\Delta E_p = (\rho_L - \rho_G)gV\delta h. \quad (5)$$

For small contact angle θ , the liquid/gas interface can be approximated by the parabola

$$y = \frac{\kappa}{2}x^2,$$

where κ is the mean curvature (inverse of the radius of curvature), and the volume by

$$\int_0^{\delta h} \pi \frac{2y}{\kappa} dy = \frac{\pi}{\kappa}(\delta h)^2 = \frac{1}{2}A_{GS}\delta h.$$

Next, since

$$\delta h \sim \frac{1}{2} \kappa r^2 \sin^2 \theta,$$

we conclude

$$A_{GS} = \frac{2}{\kappa} \pi \delta h \sim \pi r^2 \sin^2 \theta. \quad (6)$$

The difference in interfacial energies between attached and detached bubble is then

$$\Delta E_p = (\rho_L - \rho_G) g V \frac{\kappa}{2\pi} A_{GS} = (\rho_L - \rho_G) g \frac{2}{3} r^2 A_{GS}. \quad (7)$$

By comparing (5), (7) and using (6) we conclude the following condition for bubble detachment:

$$\frac{(\rho_L - \rho_G) g r^2}{\sigma_{LG}} = \frac{3}{2} (1 - \cos \theta),$$

where r is the radius of the full sphere. In terms of the radius R of the initial half-sphere, since $r = 2^{-\frac{1}{3}} R$, the critical Bond number would be

$$Bo = \frac{(\rho_L - \rho_G) g R^2}{\sigma_{LG}} = \frac{3}{2^{\frac{1}{3}}} (1 - \cos \theta). \quad (8)$$

Notice that the discussion above is restricted to small values of θ so that the critical value of Bond for detachment is $O(\theta^2)$. We will test this result numerically and, more interestingly, will find out that the parabolic dependence of the critical Bo on θ extends to all values of θ . We have simulated the evolution of a bubble that initially is a sphere section with the phase field method described previously. After a quick relaxation towards a bubble with the corresponding contact angle (that we establish a priori), the bubble evolves towards a stationary configuration for small Bo . This stationary configuration changes as Bo increases until Bo reaches a critical value and the bubble detaches.

In figure 2 we represent the critical Bond number as a function of the contact angle. The numerical simulations are fitted using a parabolic expression relating the critical Bond number with the contact angle, $Bo = l\theta^2$, being $l = 2.25$. The theoretical curve is derived as an asymptotic expression from (8), $Bo = l_{th}\theta^2$, being $l_{th} = 3/2^{1/3} = 2.38$. We find that the agreement is satisfactory given the simple arguments based on energy balance.

In figure 3 we plot some snapshots of the evolution of a bubble. We have simulated the case $Bo = 4$, and contact angle $\theta = 3\pi/5$. At those values, we are below the critical curve so we are through the process of relaxation to equilibrium without detachment.

In figure 4 we plot some snapshots of the evolution of a bubble. We have simulated the case $Bo = 15$, and contact angle $\theta = 3\pi/5$. At those values, we are above the critical curve so we are through the process of destabilization and detachment. It is noteworthy that bubbles completely detach when the contact angle is sufficiently small, but for contact angles closer to π the detached bubble does not carry all the gas and part of it is left at the substrate. Moreover, satellite bubbles do appear, much as in the case of bubbles surrounded by inviscid

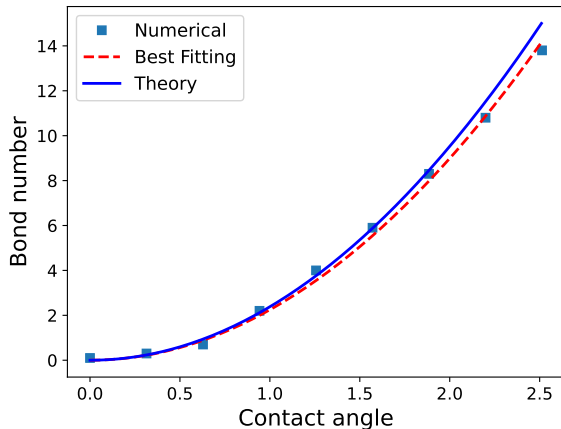


Figure 2: Bond critical number versus contact angle. Squares are numerical simulations, blue is theory and discontinuos line is the parabolic fitting of the numerical simulations $Bo = l\theta^2$, being $l_{fit} = 2.25$ and $l_{th} = 2.38$.

liquids (cf. [16]). We indeed observe this fact in the numerical simulations. We also observe that the geometry of the interface near the pinch-off point where the bubble breaks is symmetrical and close two two cones as described, for instance, in ([17]).

4 Inclined substrates

We consider in this section the effect of an inclination angle α of the substrate with respect to a substrate orthogonal to gravity. The critical Bond number increases as we can see in figure 5. In fact, for $\alpha = 30^\circ$ the critical Bond number is roughly the one corresponding to an “effective” gravity given by $g \cos \alpha$. The effect is also apparent for larger inclination angles as we can see in table 1 for different inclination angles. Again, a good approximation for the critical Bond number is the one corresponding to an effective gravity $g \cos \alpha$ but a bit larger. We can understand this as the effective combination of a new (and smaller) effective gravity together with a deformation of the contact gas/solid surface, which is no longer a circle and has a larger area, leading to a higher resistance to detachment.

In figure 6 we can see that the critical Bond number increases as compare with the theoretical value and follows the theoretical curve with an effective gravity corrected by the inclination angle.

Angle	B_o (No slope)	B_o (inclined plane 30°)	B_o (inclined plane 60°)
$\pi/5$	0.7	0.8	1.35
$3\pi/10$	2.2	2.7	4.3
$2\pi/5$	4.0	4.7	8.2
$\pi/2$	5.9	7.2	12.0
$3\pi/5$	8.3	10.0	16.8
$7\pi/10$	10.8	13.0	22.0
$4\pi/5$	13.8	16.6	30.0

Table 1: Critical B_o with different plane slopes

5 The effect of external flows

In this section we consider the bubble subjected to a external linear flow of the form

$$\mathbf{u}_{in} = W_{in} z \mathbf{e}_z,$$

imposed far away from the bubble. We can introduce a characteristic length R and velocity U , as well as the dimensionless number

$$w_{in} = \frac{W_{in} R}{U} = \frac{W_{in} R}{\sqrt{\rho_1 g R}},$$

in terms of which the condition of infinity reads

$$\mathbf{u}_{in} = w_{in} z \mathbf{e}_z.$$

Therefore, we have the following set of dimensionless numbers:

$$Bo, Re, w_{in}.$$

If we include kinetic energy into the energetic balance (with an undetermined prefactor) we arrive at the relation

$$Bo = \frac{(\rho_L - \rho_G) g R^2}{\sigma_{LG}} = \frac{3}{2^{\frac{1}{3}}} (1 - \cos \theta) - \delta w_{in}^2,$$

which is a parabolic dependence on w_{in}^2 .

Our simulations (see figure 7) indicate that Bo indeed depend cuadratically on w_{in}^2 with δ depending mildly on θ . In fact, for both small and large values of θ we found $\delta \simeq 0.25$. The dashed curves correspond to the asymptotic expression

$$Bo = \frac{3}{2^{\frac{1}{3}}} \theta^2 - \frac{1}{4} (1 - 0.35 \sin \theta) w_{in}^2.$$

The critical surface which separates the attaching-dettaching behaviour, given by

$$Bo - 3/2^{1/3}\theta^2 + 0.25(1 - 0.35 \sin \theta)w_{in}^2 = 0, \quad (9)$$

together with the numerical simulation points are depicted in figure 8. As we can see in the figure, the agreement of formula (9) with the numerical results is excellent except when θ is close to π for large velocities. The reason for this is that in that case the velocity field is able to blow a portion of the bubble before the contact line has a significant dynamics and a better approximations is given by replacing the factor $\frac{1}{4}(1 - 0.35 \sin \theta)$ by $\frac{1}{4}$, which is independent of the contact angle θ .

In figure 9 we plot various stages of the evolution of the bubble under the action of an external velocity field as computed by the phase field method. The Bond number is 15 and the initial contact angle is $3\pi/5$. The inlet velocity is a laminar flow in the right yx -plane, given by $v = -Uz$, with $U = 3$.

6 Conclusions

We have developed and implemented a phase field model for the study of the evolution and detachment from a solid substrate of a gas bubble surrounded by a viscous liquid. Three different physical conditons have been considered: 1) bubble surrounded by a quiescent viscous fluid and under the action of a vertical gravitational field, 2) bubble over an inclined plane, 3) bubble under the action of a fluid flow. We found that, in terms of dimensionless numbers, the condition for bubble detachment follows very simple laws with a strong dependence on the static Young's contact angle. These laws are quadratic with a high degree of accuracy. As a side result of our study, the phase field model is able to handle topological changes related to the pinch-off of the bubble and the formation of satellites.

If future publications we will study the detachment of bubbles that grow due to the diffusion of a gas (typically hydrogen or oxygen) inside the bubble. The gas will be produced on the solid substrate due to chemical reactions such as those associated to hydrogen production in water electrolysis. Our goal is to analyse the interplay between bubble growth and detachment and effective electrode area for chemical reaction in order to optimize the conditions for hydrogen production. In this sense, the present work helps to understand how physical parameters and mechanisms such as contact angle and external flow influence the production of gas.

Acknowledgement 1. *This work has been supported by projects TED2021-131530B-I00 and PID2022-139524NB-I00.*

References

- [1] S. M. Allen and J. W. Cahn. A microscopic theory for antiphase boundary motion and its application to antiphase domain coarsening. *Acta Metallurgica*, 27(6):1085-1095, 1979.
- [2] J. W. Cahn and J. E. Hilliard, Free energy of a nonuniform system. I. Interfacial free energy, *J. Chem. Phys.* 28, 258 (1958).
- [3] G. Caginalp. An analysis of a phase field model of a free boundary. *Archive for rational mechanics and analysis*, 92:205–245, 1986.
- [4] Q. Du and X. Feng. The phase field method for geometric moving interfaces and their numerical approximations. *Handbook of Numerical Analysis*, 21:425–508, 2020.
- [5] D. Jacqmin, Calculation of Two-Phase Navier–Stokes Flows Using Phase-Field Modeling, *Journal of Computational Physics*, Volume 155, Issue 1, 10 October 1999, Pages 96-127
- [6] V. E. Badalassi, H.D. Ceniceros, S. Banerjee, Computation of multiphase systems with phase field models, *Journal of Computational Physics* 190 (2003) 371–397.
- [7] C. Eck, M. A. Fontelos, G. Grün, F. Klingbeil and O. Vantzos, On a phase-field model for electrowetting, *Interfaces Free Bound.* 11 (2009) 259–290.
- [8] T. Qian, X.-P. Wang and P. Sheng, A variational approach to moving contact line hydrodynamics, *J. Fluid Mech.* 564 (2006) 333–360.
- [9] M. A. Fontelos, G. Grün, U. Kindelán, F. Klingbeil, Numerical Simulation of Static and Dynamic Electrowetting, *Journal of Adhesion Science and Technology* Volume 26, (1805-1824), 2012.
- [10] Z. Zhang, W. Liu and M. L. Free, Phase-Field Modeling and Simulation of Gas Bubble Coalescence and Detachment in a Gas-Liquid Two-Phase Electrochemical System, *Journal of The Electrochemical Society*, 2020 167 013532
- [11] R. Jafari and T. Okutucu-Özyurt, Phase-Field Modeling of Vapor Bubble Growth in a Microchannel, *The Journal of Computational Multiphase Flows* Volume 7, Issue 3, 143-158 (2016)
- [12] M. Farhat, F. Avellan, On the Detachment of a leading edge Cavitation, *Proceedings of the fourth international Symposium on Cavitation*, Pasadena, Ca, USA, June 2001.
- [13] W. Yin, L. Yuan ,H. Huang, Y. Cai, J. Pan, N. Sun, Q. Zhang, Q. Shu, C. Gu, Z. Zhuang, L. Wang, Strategies to accelerate bubble detachment for efficient hydrogen evolution, *Chinese Chemical Letters* 35 (2024) 108351

- [14] H. Ding, M. N. H. Gilani, P. D. M. Spelt, Sliding, pinch-off and detachment of a droplet on a wall in shear flow, *Journal of Fluid Mechanics*, Volume 644 (2010), 217-244
- [15] A. Guion , S. Afkhami , S. Zaleski, J. Buongiorno, Simulations of micro-layer formation in nucleate boiling, *International Journal of Heat and Mass Transfer*, Volume 127, Part B, December 2018, Pages 1271-1284
- [16] J. M. Gordillo and M. A. Fontelos, Satellites in the Inviscid Breakup of Bubbles, *Phys. Rev. Lett.* 98, 144503 (2007)
- [17] J. G. Eggers, M. A. Fontelos, D. Leppinen, J. H. Snoeijer, Theory of the collapsing axisymmetric cavity, *Physical Review Letters* .98, 094502 (2007).
- [18] M. Yue, H. Lambert, E. Pahon, R. Roche, S. Jemei, D. Hissel, Hydrogen energy systems: A critical review of technologies, applications, trends and challenges, *Renewable and Sustainable Energy Reviews*, Volume 146, August 2021, 111180

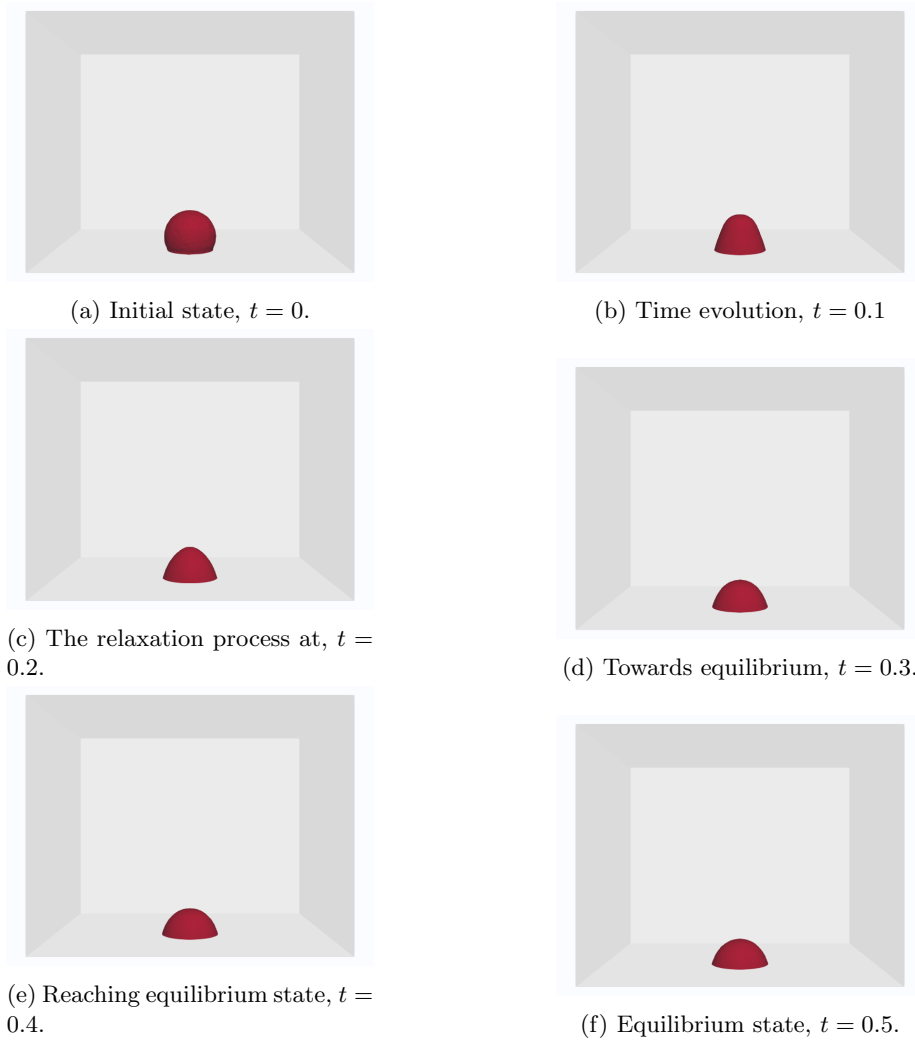


Figure 3: Numerical simulations of the evolution of a bubble with initial contact angle $3\pi/5$ and Bond number 4 (time in dimensionless units), below criticality.

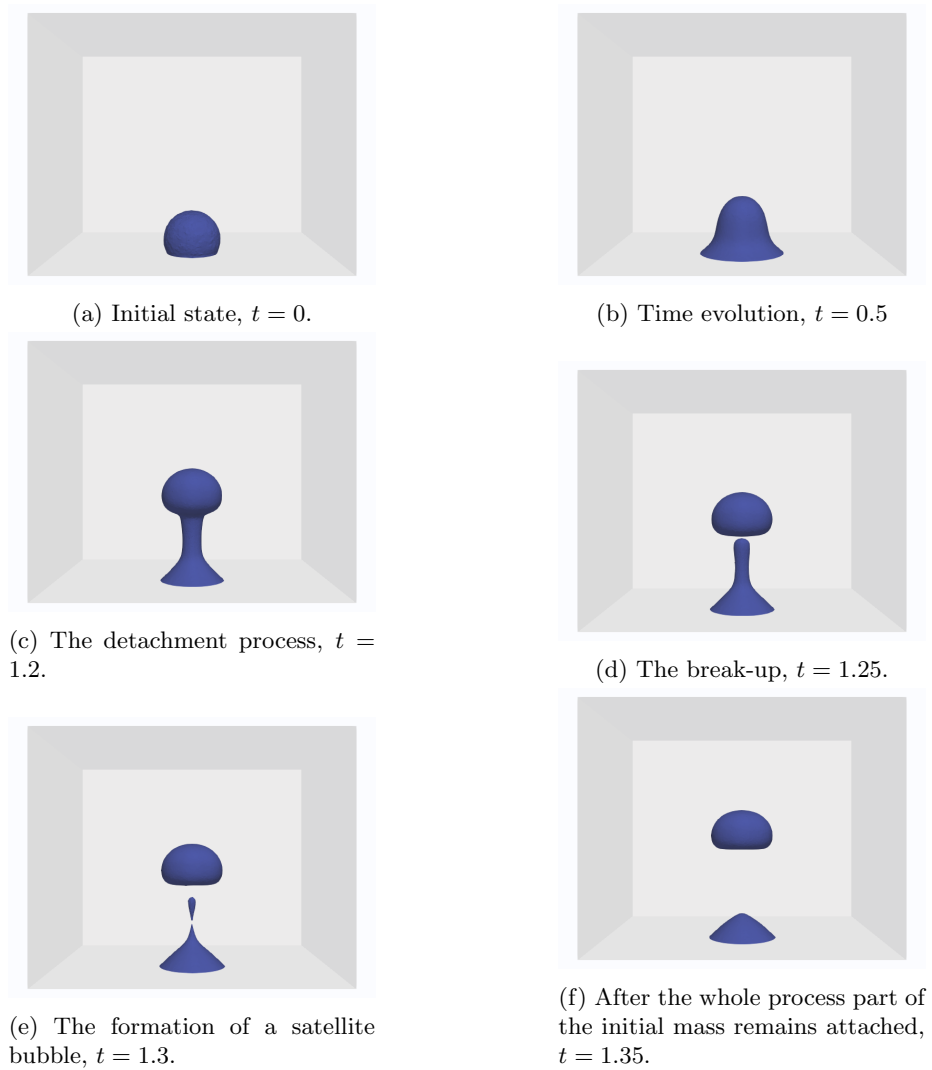


Figure 4: Numerical simulations of the evolution of a bubble with initial contact angle $3\pi/5$ and Bond number 15 (time in dimensionless units).

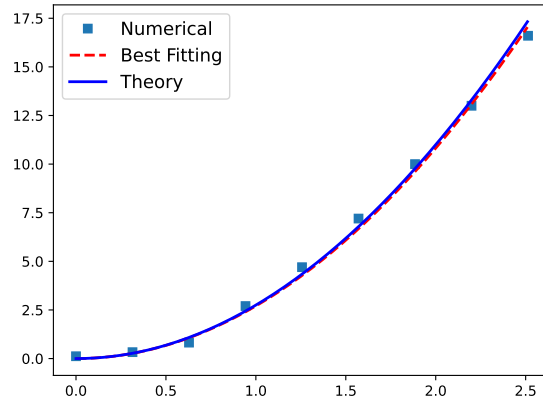


Figure 5: Bond critical number versus contact angle for an inclined substrate $\alpha = 30^\circ$. Squares are numerical simulations, blue is theory and discontinuos line is the parabolic fitting of the numerical simulations $Bo = l\theta^2$, being $l_{fit} = 2.71$ and $l_{th} = 2.38$.

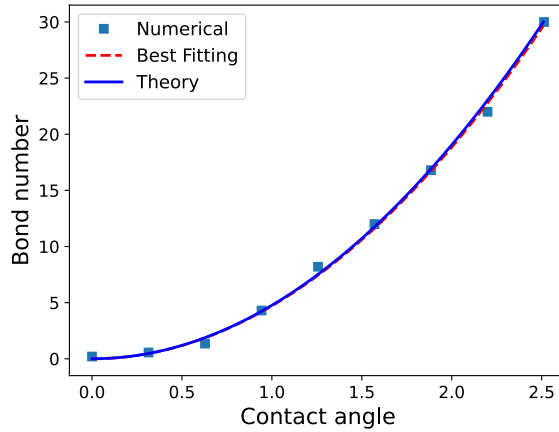


Figure 6: Bond critical number versus contact angle for an inclined substrate $\alpha = 60^\circ$. Squares are numerical simulations, blue is theory and discontinuos line is the parabolic fitting of the numerical simulations $Bo = l\theta^2$, being $l_{fit} = 4.71$ and $l_{th} = 2.38$.

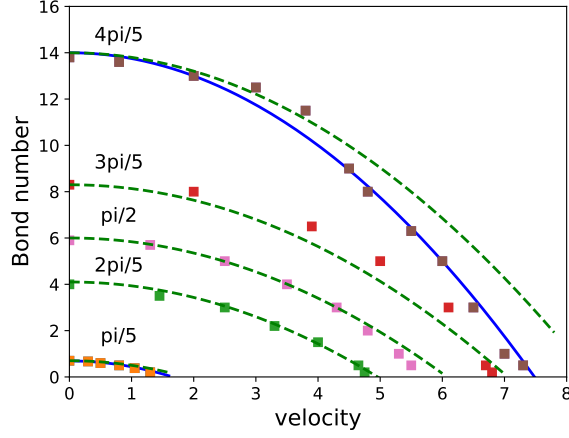


Figure 7: Bond critical number versus inlet velocities at different contact angles. Squares are numerical simulations, discontinuos lines are given by $Bo = l_{th}\theta^2 - \delta w_{in}^2$ being $l_{th} = 2.38$ and $\delta = 0.25(1 - 0.35 \sin \theta)$. The continuous line is the one with $\delta = 0.25$. For small angles ($\theta = \pi/5$) there is not difference between discontinuos and continuous curves.

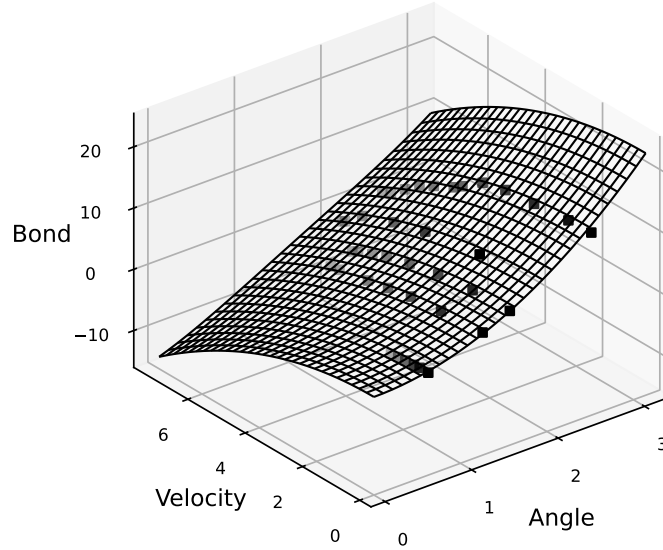
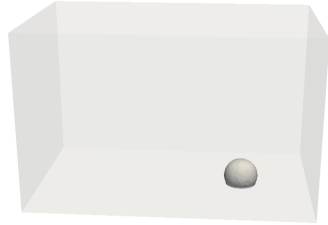
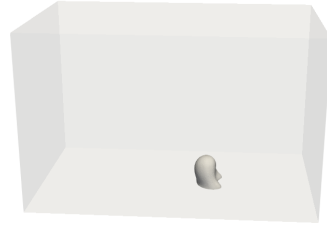


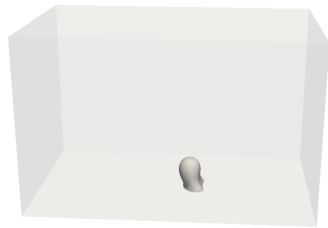
Figure 8: Critical surface. Squares points are numercial simulations, critical surface is given by $Bo - l_{th}\theta^2 + \delta w_{in}^2 = 0$, being $l_{th} = 3/2^{1/3}$ and $\delta = 0.25(1 - 0.35 \sin \theta)$.



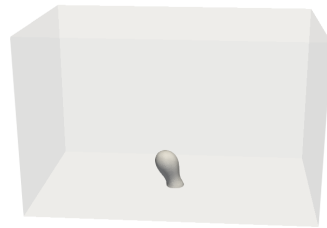
(a) Initial state, $t = 0$.



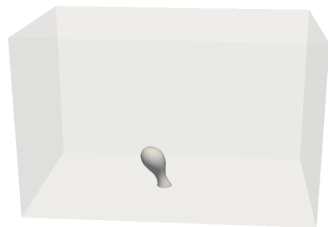
(b) Evolution under inflow, $t = 0.2$



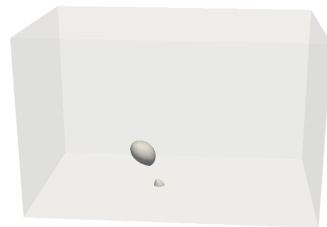
(c) Time evolution, $t = 0.3$.



(d) The detachment process, $t = 0.5$.



(e) Formation of a neck, $t = 0.6$.



(f) The break-up, $t = 0.7$.

Figure 9: Numerical simulations of the evolution of a bubble with initial contact angle $3\pi/5$, Bond number 10 (time in dimensionless units). There is an inlet linear flow $v_y = -Uz$ with $U = 3$ in dimensionless units.